Preliminary Study of the Influence of Environment Conditions on the Successive Hydrogenations of CO

ARTICLE *in* THE JOURNAL OF PHYSICAL CHEMISTRY A · FEBRUARY 2010

Impact Factor: 2.69 · DOI: 10.1021/jp909600q · Source: PubMed

Claire Pirim
Université des Sciences et Technologies de…

P. Parent
French National Centre for Scientific Resea…

Julien Pilme
Pierre and Marie Curie University - Paris 6

Preliminary Study of the Influence of Environment Conditions on the Successive Hydrogenations of CO†

C. Pirim and L. Krim*

Laboratoire de Dynamique, Interactions et Réactivité, Université Pierre et Marie Curie-Paris 6, CNRS, UMR 7075, Case Courrier 49, Bat F 74, 4 Place Jussieu, 75252 Paris Cedex 05, France

C. Laffon and Ph. Parent

Laboratoire de Chimie Physique, Matière et Rayonnement, Université Pierre et Marie Curie-Paris 6, CNRS, UMR 7614, 11 rue Pierre et Marie Curie, 75231 Paris Cedex 05, France

F. Pauzat,‡ J. Pilmé,‡,§ and Y. Ellinger‡

Laboratoire de Chimie Théorique, Université Pierre et Marie Curie-Paris 6, CNRS, UMR 7616, F-75005, Paris, France, and Université de Lyon 1, F-69373 Lyon, France

Received: October 7, 2009; Revised Manuscript Received: January 6, 2010

The successive hydrogenation of CO has been investigated by two methods. The first is hydrogenation of a CO surface. The second is co-injection of CO molecules and H atoms. Both methods have been performed at 3 and 10 K. In the first method, the interaction of H atoms with solid CO at 10 K shows that CO is consumed to form H_2CO and CH_3OH. No trace of species such as HCO and CH_3O is detected. No product was observed when the same experiment was performed at 3 K. In the second method, when H and CO are codeposited at 10 K, HCO and CH_3O are observed. In fact, the yield of these intermediate species depends on the amount of the H radicals interacting with CO molecules. At 3 K, the presence of H_2 in the solid screens the hydrogenation reaction. This causes a termination for the reaction in the stage of the formation of HCO and H_2CO. At 10 K, H_2 cannot condense, and the reaction between CO and H is total. In this case, species such as HCO, H_2CO, CH_3O, and CH_3OH are observed.

1. Introduction

Carbon monoxide (CO) is the most abundant molecule observed in the interstellar medium[1] (ISM) after H_2 and is largely present in both the gas and solid phases. Its presence, characterized by the 4.67 μm IR absorption, seems ubiquitous at the surface of dust grains in dense ISM.[2–4] The fraction of CO that is not frozen on grains plays an important role in mapping molecular clouds in galaxies because CO pure rotational transitions are the best existing probe for the distribution and physical condition of the cool matter in the universe.[5] This is the reason why several groups have focused their work on the understanding of H_2−CO van der Waals complexes and collisional excitation.[6–8] In addition to being a tracer of the molecular population in the gas phase, CO is also a key molecular step in the synthesis of many organic molecules. One of these reactions, which has been the center of numerous studies, is the process of successive hydrogenations of CO (reaction 1)

$$CO \xrightarrow{1} HCO \xrightarrow{2} H_2CO \xrightarrow{3} H_3CO \xrightarrow{4} CH_3OH \qquad (1)$$

As described in reaction 1, products of the reaction H + CO are precursors to the formation of methanol,[9] which can also lead to the formation of the COOH acid group in the ISM. This process (reaction 1) has been studied experimentally and theoretically, mostly in solid CO, although more recent investigations have been carried out using analogues of dust grain surfaces.[10–12] To study the hydrogenation of icy-grains analogues, different detections techniques have been used such as mass spectrometry[13] or Fourier transform infrared spectrometry[14] (FT-IR). The electron paramagnetic resonance (EPR) has also been used to monitor the co-condensation of CO and H,[15] where HCO and CH_3 radicals were detected. Recent studies consisted of spraying an analogue of dust grain surface with H atoms at a temperature range of 10−20 K. The goal was to study the interaction of H atoms with CO−ice surfaces[16] and the reaction rates of H_2CO and CH_3OH formation.[17] Parameters such as temperature and isotopic effects have been studied during the hydrogenation of CO on ice surfaces.[18] Previous FT-IR studies have characterized some of the free radicals appearing in the CO hydrogenation process (reaction 1). Therefore, HCO[19,20] and CH_3O[21] frequencies are now precisely referenced.

The aim of the present work is not only to understand the role and evolution of the intermediate species formed in the reactions of successive hydrogenations of CO (reaction 1) but also to determine the conditions for promoting each step in this mechanism. This work is focused on the preliminary results obtained by co-injection of CO molecules and H atoms using FT-IR spectroscopy. The experiment of successive hydrogenation of a CO surface, similar to those previously reported by other groups, has been reproduced for comparison. The technical background, experimental and computational, is summarized in

† Part of the "Benoît Soep Festschrift".

* To whom correspondence should be addressed. E-mail: lahouari.krim@upmc.fr.

‡ Université Pierre et Marie Curie-Paris 6.

§ Université de Lyon.

10.1021/jp909600q

Section 2. The experiments and associated calculations are reported in Section 3. The discussion of the results is presented in Section 4, and Section 5 summarizes our conclusions.

2. Technical Background

2.1. Fourier Transform Infrared Spectrometry Study. The atomic hydrogen sprayed over CO is produced by a microwave-driven atom source (SPECS PCR-ECS). This source uses a microwave discharge to generate, through the electron cyclotron resonance (ECR) phenomenon, a gas plasma in a chamber fed with molecular hydrogen. H_2 gas is injected at 1 bar, and the pressure of the chamber during operation of the atom source is 10^{-5} mbar. The gas leaving the chamber through the apertures is a combination of both atomic and molecular hydrogen H/H_2 (15/85%). A tube has been added after the apertures to eliminate UV photons. The partition of atomic and molecular hydrogen monitored is the same with or without the UV-blocking tube, and thus it has no influence on the H atom recombination yield. A cryogenic metal mirror, where chemical species are condensed at low temperatures, is positioned perpendicularly, 7 cm away from the H/H_2 beam exit (flux about 10^{14} atoms cm^{-2} s^{-1}). The CO + H samples were prepared by co-condensing $CO/H/H_2$ mixtures onto the cryogenic metal mirror maintained between 3 and 10 K, depending on the experiment. This temperature is kept stable using a pulsed tube closed-cycle cryogenerator (Cryomech PT405). The setup was evacuated at 7×10^{-7} mbar before refrigeration of the sample holder. High-purity molecular hydrogen ("Air liquide"; 99.995%) and CO (Matheson; 99.5%) were used to prepare the CO + H/H_2 mixture.

Infrared spectra of the resulting samples were recorded in the transmission-reflection mode between 4500 and 500 cm^{-1}, with a resolution of 0.5 cm^{-1}. The instrument used is a Bruker 120 FTIR spectrometer equipped with a KBr/Ge beamsplitter and a liquid N_2-cooled narrow band HgCdTe photoconductor. The incidence angle of the IR beam in the spectrometer is 8°. Bare mirror backgrounds, recorded from 4500 to 500 cm^{-1} prior to sample deposition, were used as references in processing the sample spectra. Midinfrared absorption spectra were collected on samples through a KBr window mounted on a flange, separating the interferometer vacuum (10^{-3} mbar) from that of the cryostatic cell (10^{-7} mbar). The spectra were subsequently subjected to baseline corrections to compensate for infrared light scattering and interference patterns. The infrared experimental methods have been previously described.[22]

First, a micrometer thick pure CO ice was obtained by condensing CO gas onto the mirror maintained at 10 K. With the deposition rate being 10 μmol/cm^2·min, a dosing time of 1 min is enough to give a film thickness of few micrometers, but the exact thickness was not measured directly. The CO surface was then bombarded by H atoms. The same experiment was performed later on at 3 K.

To enhance the amount of CO molecules exposed to H, we have also performed samples where CO and H were coinjected at 3 or 10 K.

Finally, annealing was performed stepwise up to 50 K for each of the experiments described above.

2.2. Computational Study. To help with these investigations, specific calculations were performed. They were essentially targeted on the most plausible species, and complexes that can be reasonably formed in these experiments and for which experimental data are not available. Post Hartree−Fock (HF) methods using Möller-Plesset (MP) perturbation theory at second (MP2) and fourth (MP4) orders were employed with a correlation-consistent[23–25] cc-pVQZ basis set. Each structure taken under consideration was fully optimized and verified to be a stationary point by vibrational analysis. The energy differences between calculated complexes and isolated components were calculated taking into account the contribution of the zero point energy (ZPE). The frequencies and intensities were calculated in the harmonic approximation at the MP2 level. Because only the shifts of the CO band from the reference molecules CO, HCO, and H_2CO were of interest in this present study, we did not apply any scale factor to the frequencies. These factors are used as a surrogate to the error coming from the missing part of correlation and anharmonicity. In this case, these errors are very likely of the same order for all species considered, so they should compensate in the differences.

All calculations were performed using the GAUSSIAN03 package.[26]

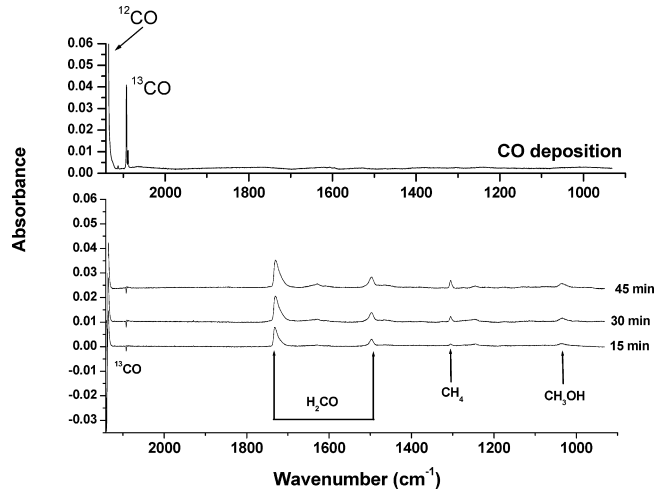

Figure 1. (top) Solid CO spectrum at 10 K. (bottom) IR spectrum of the CO surface exposed to H atoms during 45 min. Negative and positive peaks correspond to decrease and increase in the absorption spectra, respectively, under H exposure.

3. Results

3.1. Hydrogenation of Pure CO Ice at 10 and 3 K. The hydrogenation at 10 K of a several micrometer pure CO ice is shown in Figure 1. The sample is prepared by depositing pure CO gas for one minute onto a cryogenic metal mirror maintained at 10 K. The CO ice is then bombarded with a mixture of H/H_2 during 45 min and spectra are recorded every 15 min.

The spectrum shown in Figure 1 (top) corresponds to the deposition of several layers of CO. Both ^{12}CO and ^{13}CO isotopomers are present. The former band saturates with an absorbance value >1, whereas the absorption band of the ^{13}CO has an intensity (on absorbance scale) of 0.04. Therefore, the band of ^{13}CO is chosen to represent CO evolution under H bombardment.

As the CO ice is exposed to H atoms, species such as H_2CO[27,28] (1740; 1500 cm^{-1}) and CH_3OH[28] (1030 cm^{-1}) are formed. The intensity of their bands increases with time of exposure to H atoms, whereas the intensity of the CO band decreases. The changes in the absorption spectra after H exposure are represented in Figure 1 (bottom). Positive and negative absorbance peaks correspond to an increase or decrease in absorbance intensities, respectively, compared with the initial CO layer (Figure 1 (top)).

We also detected a weak signal corresponding to CH_4[28] (1300 cm^{-1}) and identified as local contamination from the H atom source.

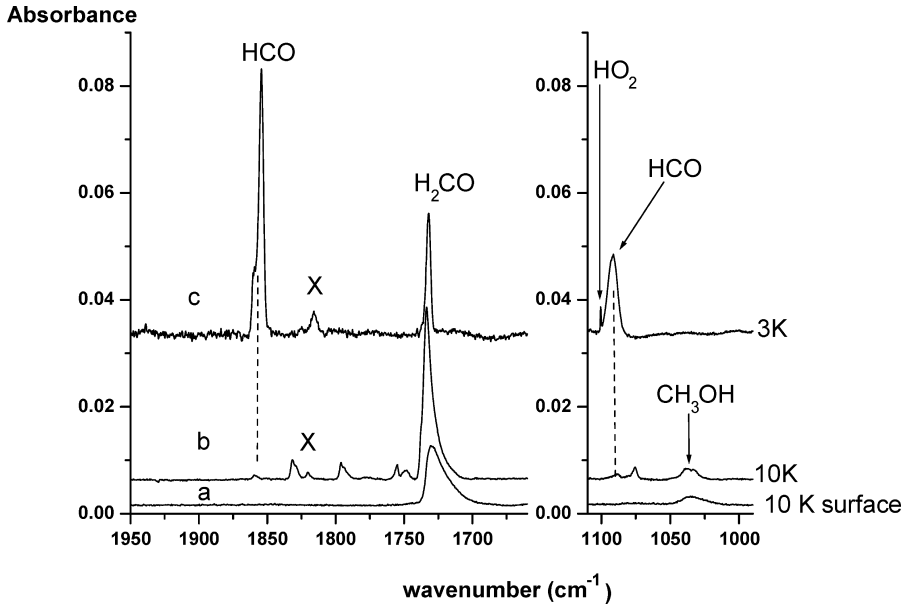

Figure 2. CO stretching and HCO bending spectral region. Comparison of: (a) hydrogenation of a CO surface at 10 K during 45 min; (b) co-injection of (CO + H) at 10 K during 8 min; (c) co-injection (CO + H) at 3 K during 8 min. HO_2 ν_3 mode can be seen at 1100 cm^{-1}. This species is produced while the H atom source is running. The species labeled X corresponds to the band located at 1816 cm^{-1} and is observed at both 3 and 10 K.

Lastly, no HCO[19,20] (ν_{CO} band located around 1850 cm^{-1}) is formed in this experiment. This corroborates the results reported by Watanabe et al.[29] regarding a CO ice surface of several monolayers irradiated by H atoms at 10 K.

No product was obtained at 3 K when exposing the micrometer thick CO ice to H atoms. Indeed, at this temperature, neither HCO nor H_2CO is observed after 45 min of H exposure.

3.2. Co-Injection of H and CO at 10 and 3 K. The spectra given in Figure 2 show the results of a co-condensation of CO and H atoms at 10 and 3 K. They are compared with the previous experiment done on a CO−ice surface. The spectral region presented here is limited to the absorption bands of interest to this study.

A first general trend is observed: contrary to hydrogenation of the CO ice at 10 K that yields only H_2CO and CH_3OH (Figure 2a), co-injections of CO and H atoms at 10 or 3 K allow a greater number of species to be formed.

The most striking change appears on the 3 K spectrum (Figure 2c) with the emergence of the signature of the transient HCO radical (at 1854 cm^{-1}) that is stronger than that of the stable H_2CO molecule (at 1732 cm^{-1}). Figure 2c also shows that neither CH_3O nor CH_3OH are formed at this temperature, as illustrated by the absence of their characteristic frequencies around 1030 cm^{-1}.

At 3 K, the hydrogenation reaction of CO seems to be blocked at the level of the formation of HCO and H_2CO, with $S_{HCO} > S_{H_2CO}$. S_{HCO} and S_{H_2CO} are the integrated areas of HCO (1854 cm^{-1}) and H_2CO (1732 cm^{-1}) absorption bands, respectively.

The results of the codeposition of H and CO at 10 K are shown in Figure 2b. We distinguish the characteristic absorption bands of HCO at 1859 cm^{-1}, that of H_2CO at 1733 cm^{-1}, and those of CH_3OH and CH_3O around 1030 cm^{-1} that were absent at 3 K. This spectrum (Figure 2b) also shows that unlike the experiments performed at 3 K the reaction of CO hydrogenation at 10 K is total, and all species, HCO, H_2CO, CH_3O, and CH_3OH, are observed. However, S_{HCO} is much lower than S_{H_2CO}.

Moreover, at both 10 and 3 K, new species appear between the absorption bands of HCO and H_2CO. More precisely, five new bands appear at 1830, 1820, 1794, 1755, and 1748 cm^{-1} when the experiment is performed at 10 K (Figure 2b), and only one band appears at 1816 cm^{-1} when the experiment is done at 3 K (Figure 2c). It seems reasonable to wonder whether these new absorption bands could be linked to complexes or molecules formed by the reaction of the HCO radical with its environment. For instance, it can be noted that the two bands around 1750 cm^{-1} are quite close to those observed for the CO vibrations in the glyoxal spectrum.[30] Future work will be dedicated to the characterization of these species. In this first report, we focus on the species labeled X, corresponding to the band located at 1816 cm^{-1} and observed at both 3 and 10 K. The species absorbing at 1816 cm^{-1} is labeled X from here on.

Figure 3a shows the evolution of the infrared fingerprints of HCO and H_2CO during the co-injection of H and CO, at 3 K. H atoms and CO are coinjected for eight minutes and spectra are recorded every minute. In this experiment, the reaction time is limited to 8 min to avoid sample opacity to the infrared beam. Figure 3b displays the evolution of the integrated areas of the IR absorption bands (S) as a function of the H exposure time for ^{12}CO, X, HCO, H_2CO, and H_2[31] (ν_{H-H} absorption band of solid H_2 at 3 K located around 4200 cm^{-1}). This Figure shows that HCO, H_2CO, and X's integrated areas increase linearly with time and that these products are formed immediately at the start of the CO and H co-injection. Indeed, no phenomenon involving a chemical conversion such as HCO → X, HCO → H_2CO, or H_2CO → X is observed in this kinetic study.

The sample obtained at 3 K is then annealed by a stepwise increase in the temperature up to 10 K (Figure 4). Until the temperature reaches 10 K, spectra are recorded at 3 K; that is, between each increasing temperature step, the sample is cooled down to 3 K. Therefore, spectra are recorded at the same temperature and are comparable. When the temperature of 10 K is reached, the spectra are monitored at 10 K for comparison with experiments performed directly at 10 K.

When increasing the temperature from 3 to 6 K, IR intensities of HCO and H_2CO absorption bands remain constant. Around 6 K, solid H_2 desorbs. The ν_{H-H} absorption band located around 4200 cm^{-1} disappears completely at 6.5 K. This spectral region is not shown in the Figures. The intensities of HCO and H_2CO

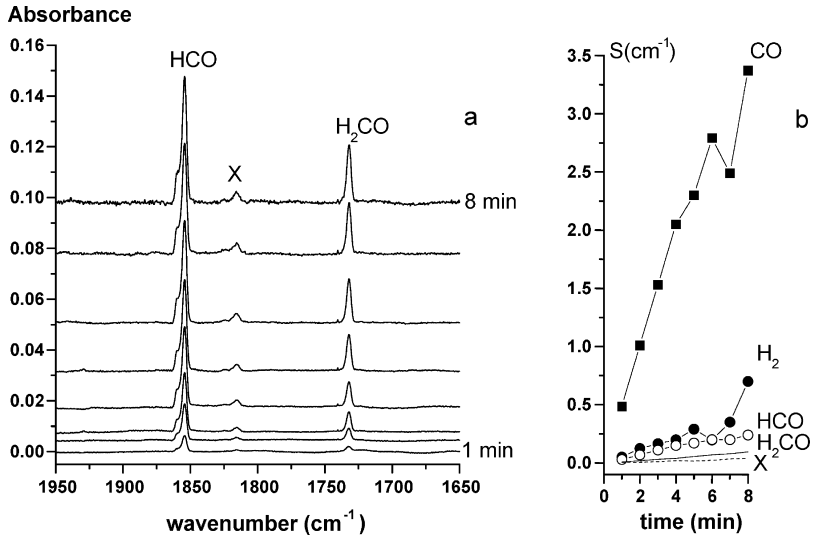

Figure 3. (a) (CO + H) co-injection at 3 K during 8 min with spectra monitored every 1 min. CO stretching spectral region. Species labeled X appears at 1816 cm^{-1}, HCO = 1854 cm^{-1}, H_2CO = 1732 cm^{-1}. (b) Kinetics of the three main products: HCO (1854 cm^{-1}), X (1816 cm^{-1}), and H_2CO (1732 cm^{-1}).

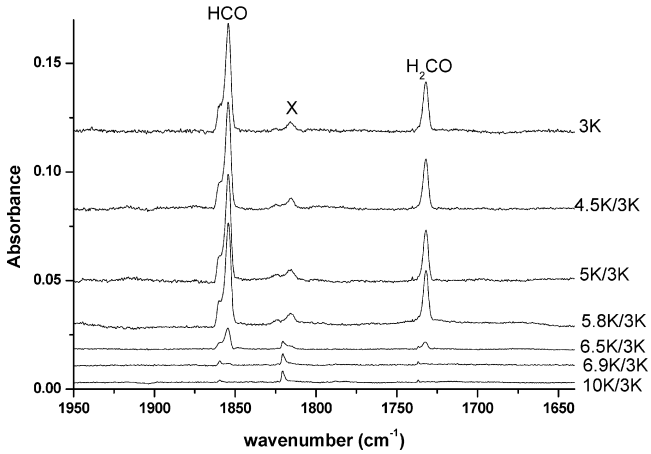

Figure 4. CO + H co-injection experiment: annealing effects. CO stretching spectral region.

infrared absorption bands are clearly decreasing between 6 and 10 K. On the contrary, the intensity of the $2\nu_{CO}$ absorption band does not decrease between 6 and 10 K like that of HCO and H_2CO. Indeed, the high concentration of CO in the sample involves the presence of a mixed-matrix (H_2 + CO) between 3 and 6 K. Nevertheless, because of H_2 desorption around 6 K, the matrix becomes only a CO matrix at higher temperatures. This point will be discussed later on in Section 4.

The shape of species labeled X evolves when the temperature is increased. The splitting of the peak into two components (1816 and 1820 cm^{-1}) becomes more and more visible between 3 and 6 K. When H_2 desorption temperature is reached (T > 6.5 K), only the left component (1820 cm^{-1}) persists. The comparison with the codeposition performed directly at 10 K is made in Figure 5. One can see that during the annealing process, HCO absorption decreases until it reaches an intensity comparable to that of the spectra recorded directly at 10 K. No conversion of HCO to H_2CO or to CH_3OH is observed by heating the system. This means that H and H_2 molecules evaporating from the matrix do not react with HCO to form H_2CO, CH_3O, or CH_3OH. Indeed, when the temperature increases between 3 and 10 K, the band intensities of HCO and H_2CO decrease simultaneously, and no trace corresponding to CH_3O or CH_3OH is observed.

The species X is present in both spectra (Figure 5), but its absorbance value is greater when the experiment is performed at 3 K and then annealed to 10 K. Figure 5 shows a band at 963 cm^{-1}, whose relative intensity has the same variation pattern with temperature as that at 1820 cm^{-1}. We assume that this peak belongs to the same chemical species X.

The other new bands located at 1830, 1794, 1755, and 1748 cm^{-1} appear only when CO and H atoms are co-condensed at 10 K. They are not formed by heating the experiment above 3 K. These species are still under investigation.

3.3. Computational Study and Tentative Characterization of the New Bands Observed. The species comprising the system at 3 K are H, H_2, CO, HCO, and H_2CO. Consequently, some of these five radicals or molecules should be involved in the formation of the new species appearing at 3 K, either as a combination of themselves (complexes or new molecules) or as dimers. The aim of this theoretical study is to help with the characterization of the new species that was formed.

Vibrational frequencies of $(HCO)_2$ and $(H_2CO)_2$ have been determined in rare gas matrix isolation.[13,32,33] We do not observe any absorption band of $(HCO)_2$ dimer or $(H_2CO)_2$ in our experiment performed at 3 K. Indeed, at 3 K, the IR signal of HCO or H_2CO is too low to permit the formation of complexes such as $(HCO)_2$, (HCO)−(H_2CO), and $(H_2CO)_2$. Moreover, at this very low temperature, there is no migration of trapped species such HCO or H_2CO in the mixed-matrix, formed mainly by CO and H_2 molecules. Therefore, molecular interactions such as HCO−CHO, HCO−H_2CO, or H_2CO−H_2CO are unlikely to be supported.

Because CO and H_2 are coinjected with a similar flux, complexes such as $HCO(CO)_n$, $H_2CO(CO)_n$, and $HCO(H_2)_n$, $H_2CO(H_2)_n$ are more likely to be formed. Because no experimental study is available on these complexes, quantum calculations were performed.

$HCO(H_2)_n$. Calculations show that these complexes are stable and can be formed in almost athermic reactions (Table 1). The calculated vibrational shift of the ν_{CO} absorption of $HCO(H_2)_{n=1-3}$ is at most 4 cm^{-1} (Table 1). This is about the peak's width of the ν_{CO} band of HCO, measured in our spectra at 3 K (Figure 4). Indeed, experimentally, the presence of weakly bound complexes appears as a simple widening of the absorption bands of the monomers, which is not conclusive.

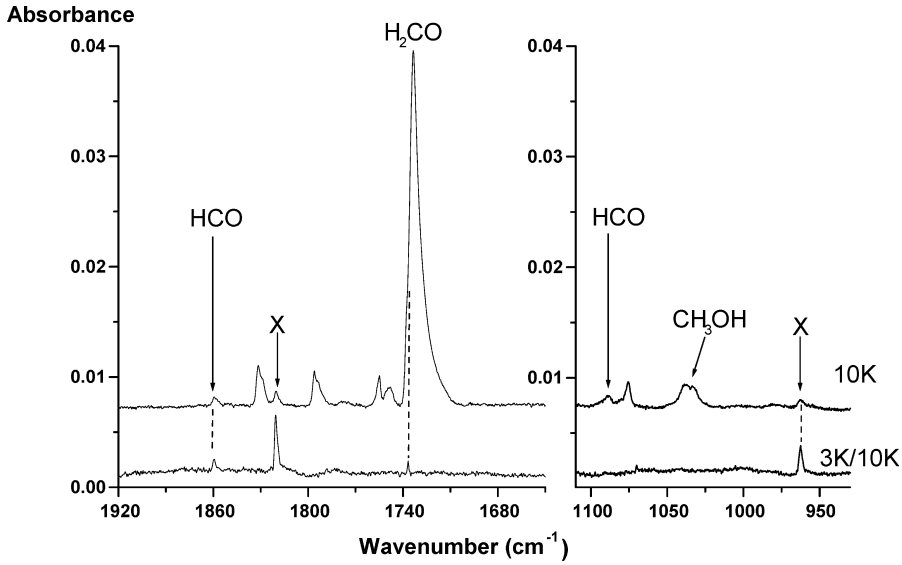

Figure 5. Comparison between (CO + H) co-injection experiments: CO stretching and HCO bending spectral region. (top) Performed directly at 10 K. (bottom) Performed at 3 K and annealed up to 10 K. Bands labeled X have the same variation pattern and could correspond to the same chemical species.

TABLE 1: HCO and H_2 Complexes Calculated at the MP2/ccpVQZ Level[a]

Molecules and complexes	ΔE (kcal/mol) Without/With ZPE	d_{C-O} (Å)	Δν(CO) (cm^{-1})	I(CO) (km/mole)
HCO		1.1764		63
HCO : H_2 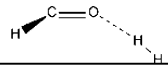	-0.6/+0.5	1.1765	0	63
HCO : 2(H_2) 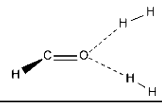	-1.0/+0.3	1.1767	+4	68
HCO : 3(H_2) 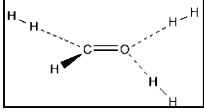	-1.3/+1.1	1.1765	+3	69

[a] ΔE is the energy difference between the complex (HCO:nH_2) and its isolated components (HCO + nH_2), $\Delta\nu$(CO) is the shift of the CO stretching frequency taking the value in isolated HCO as reference, I(CO) is the absolute intensity of the CO stretching frequency, and d_{C-O} is the bond length in the optimized structures.

$H_2CO(H_2)_n$ and $H_2CO(CO)_n$. The binding energies (practically athermic) and the vibrational frequency shifts are reported in Tables 2 and 3 for these species. The same phenomenon as the one previously described is observed with $H_2CO(H_2)_n$ and $H_2CO(CO)_n$. A very small vibrational shift is calculated between the H_2CO monomer vibrational frequencies and those of $H_2CO(H_2)_n$ or $H_2CO(CO)_n$ complexes.

Experimentally, the species labeled X is red shifted by 34 cm^{-1} from that of the HCO monomer (Figure 4). Yet, preliminary calculations on the interaction of (HCO, H_2CO) and (H_2, CO) showed that the shifts induced by the formation of complexes such as $HCO(H_2)_n$ and $H_2CO(H_2)_n$ trapped in CO matrix, or complexes as $H_2CO(CO)_n$ trapped in H_2 matrix, were too small to correspond to the species X.

HCO(CO). Contrary to the preceding situation, the interaction between HCO and CO cannot be characterized as a weak interaction. Indeed, HCO and CO can establish a true CC chemical bond and form a glyoxyl radical. Again, to our knowledge, no data were available regarding the glyoxyl radical. Therefore, calculations were performed to study this molecule and are summarized in Table 4.

To shed light on the new species emerging in the reaction process, it is interesting to assess the ν_{CO} bands shifts with respect to a well-characterized intermediate, HCO. For glyoxal, there is a red shift of the ν_{CO} band by ~120 cm^{-1}, whereas for the glyoxyl radical, we find a theoretical red shift by 23 cm^{-1}. It has to be noted that in this last radical the ν_{CO} vibration considered above does not correspond to the stretching of the

TABLE 2: H_2CO and H_2 Complexes Calculated at the MP2/ccpVQZ Level[a]

Molecules and complexes	ΔE (kcal/mol) Without/With ZPE	d_{C-O} (Å)	Δν(CO) (cm^{-1})	I(CO) (km/mole)
H_2CO		1.207		67
$H_2CO : H_2$ 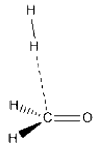	-1.0/+0.1	1.206	0	62
$H_2CO : 2(H_2)$ 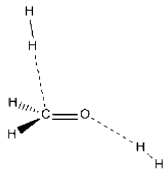	-1.8/+0.9	1.207	-4	54
$H_2CO : 3(H_2)$ 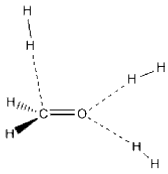	1.7/+0.9	1.207	-4	53

[a] ΔE is the energy difference between the complex ($H_2CO{:}nH_2$) and its isolated components ($H_2CO + nH_2$), $\Delta\nu$(CO) is the shift of the CO stretching frequency taking the value in isolated H_2CO as reference, I(CO) is the absolute intensity of the CO stretching frequency, and d_{C-O} is the bond length in the optimized structures.

CO in the HCO part but to the stretching of the other CO. This can be explained on electronic grounds: the HCO part of HCOCO has the same electronic characteristics as HCO in H_2CO, whereas the CO part bears the open shell radical center and consequently resembles the isolated radical HCO. In IR spectra recorded at 3 K, species X's absorption band is red-shifted by 34 cm^{-1} from that of the HCO monomer. The calculated vibrational shift between the ν_{CO} frequency of HCO when interacting with CO is close to the spectral shift measured for the band corresponding to species X; this suggests that the glyoxyl radical could correspond to the species labeled X and should go under further investigation. More experimental studies using isotopic substitution, H/D and $^{12}C/^{13}C$, are currently being undertaken to better characterize this new species. Other possibilities are currently under investigation, namely, the products possibly resulting from the addition of CO, HCO, or H_2CO to the glyoxyl radical, leading to the formation of transient free radicals such as $HCO(CO)_n$, $HOCCH_2O$, HOCCHOH, and $HOCCH_2OH$. New information relative to these species will be discussed in a forthcoming paper.

4. Discussion

In this study, two types of experiments were performed. The first experiment consists of bombarding H atoms on a CO ice surface condensed onto a mirror. In the second experiment, CO molecules and H atoms were co-condensed onto a mirror. Both types of experiments were carried out at 3 K as well as 10 K. From the results obtained, CO successive hydrogenations (reaction 1) seem to be largely influenced by environment conditions.

4.1. Surface Bombardment Experiments. The results obtained at 10 K on micrometer thick CO surface are similar to those obtained by Watanabe's group[34] when exposing the surface of a few monolayers of CO to a hydrogen atom beam. The intensity of H_2CO and CH_3OH absorption bands increases with H exposure. We observed that H_2CO and CH_3OH absorption values are saturated after almost 30 min of exposure to H atoms. This is likely due to the CO surface being coated with products of the reaction H + CO.

HCO is not observed in our spectra, as in the Watanabe's experiment; this indicates that under such experimental conditions, the hydrogenation on the CO surface easily goes on to form the stable molecules H_2CO and CH_3OH.

Moreover, when exposing a micrometer thick CO ice to H atoms at 3 K, no other spectral signature has been identified. Indeed, the hydrogen beam exiting the microwave discharge is composed of a fraction of hydrogen atoms and molecular hydrogen, H/H_2 (15/85%). At 3 K, H_2 molecules condense onto the mirror, shielding the CO surface. Therefore, H atoms cannot react with CO and, under such condition, reaction CO + H does not take place.

4.2. Co-Injection Deposition Experiments. The co-injection CO + H reaction forms intermediate species HCO and (CH_3O,

TABLE 3: H_2CO and CO Complexes Calculated at the MP2/ccpVQZ Level[a]

Molecules and complexes	ΔE (kcal/mol) Without/With ZPE	d_{C-O} (Å)	Δν(CO) (cm^{-1})	I(CO) (km/mole)
H_2CO		1.207		67
CO		1.191		35
H_2CO : CO 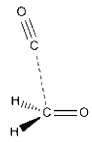	-1.2/-0.6	1.206 (H_2CO)	+1	67
		1.131 (CO)	+3	35
H_2CO : 2(CO) 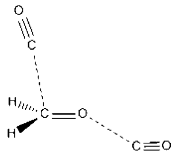	-3.0/-1.9	1.207 (H_2CO)	-5	58
		1.132 (CO)	+1/+2	34/32
H_2CO : 3(CO) 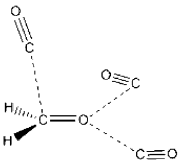	-4.6/-3.5	1.207 (H_2CO)	+5	48
		1.132 (CO)	+18/+24/+25	34/32/33

[a] ΔE is the energy difference between the complex (H_2CO:nCO) and its isolated components (H_2CO + nCO), $\Delta\nu$(CO) are the shifts of the CO stretching frequencies in the complexes with respect to the same frequencies in isolated H_2CO/CO, respectively, I(CO) is the absolute intensity of the corresponding CO stretching frequency, and d_{C-O} is the bond length in the optimized structures. For each complex, upper entries ($\Delta\nu$, I) refer to the H_2CO fragment; lower entries refer to CO diatomics.

TABLE 4: (HCO:CO) Complex Calculated at the MP2/ccpVQZ Level[a]

Molecules and complexes	ΔE (kcal/mol) Without/With ZPE	d_{C-O} (Å)	Δν(CO)/HCO (cm^{-1})	Δν(CO)/CO (cm^{-1})	I(CO) (km/mole)
HCO		1.176			63
CO		1.191			35
HCO-CO (Glyoxyl radical) 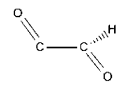	-0.58/+4.3	1.176(HCO)	- 23	- 205	74
		1.191(CO)	+385	+180	581

[a] ΔE is the energy difference between the complex (HCO:CO) and its isolated components (HCO + CO), $\Delta\nu$(CO) are the shifts of the CO stretching frequencies in the complexes with respect to the same frequencies in isolated HCO/CO, respectively, I(CO) is the absolute intensity of the corresponding CO stretching frequency, and d_{C-O} gives the bond length in the optimized structures. Upper entries ($\Delta\nu$, I) refer to the HCO fragment; lower entries refer to CO diatomics.

CH_2OH) corresponding to different steps of the CO hydrogenation process (reaction 1).

These intermediate species are not observed with the previous surface experiment. Because the yield of this reaction depends greatly on temperature variations and on the ratio of H/H_2, changing the CO deposition temperature will promote specific intermediate species of the CO + H reaction:

(i) CO + H co-injection performed at 10 K yields HCO (weak IR intensity) and both H_2CO and CH_3OH (higher IR intensities than HCO). Some new species are also observed with IR signatures between HCO and H_2CO absorption bands in the ν_{CO} spectral region and are still under investigation. It can be suggested that a temperature of 10 K enhances the mobility of the adsorbed species, which favors the formation of new compounds. (ii) CO + H co-injection performed at 3

K freezes the CO hydrogenation process at the first limiting step of the reaction. Therefore, only HCO and H_2CO (weaker IR intensity than HCO) are produced. No trace of H_3CO and CH_3OH is observed at this temperature.

This can be easily explained by the fact that at very low temperatures, molecular hydrogen condenses with CO molecules to form a micromatrix that isolates HCO. Indeed, solid H_2 forms a screen between HCO and other H atoms supplied by the atomic source. Therefore, only HCO and a few H_2CO molecules are formed and isolated.

Then, HCO and the few H_2CO molecules are no longer involved in the process of CO hydrogenation. Moreover, the migration of species trapped in the H_2 or CO matrix is facilitated at higher temperatures than 3 K, and reactions such as HCO + H + H + H are not favored at 3 K.

It should also be noted that only one new species is formed (peak at 1816 cm^{-1}) at 3 K. Its intensity varies with that of HCO, suggesting that this species could be a complex like $(HCO)(CO)_n$. The co-injection carried out at 3 K is annealed stepwise (1 K intervals) up to 10 K. During this process, both HCO and H_2CO intensities decrease, and no conversion of HCO into H_2CO is observed. In the temperature range 3−10 K, the absorption band intensities in the HCO and H_2CO region are decreasing, and the band shapes are shifting. This is probably due to the disappearance of species such as $HCO\cdot(H_2)_n$ and $H_2CO\cdot(H_2)_n$ due to H_2 desorption. Indeed, the high concentration of CO in the sample involves the presence of a mixed-matrix (H_2+CO) between 3 and 6 K. Nevertheless, because of H_2 desorption around 6 K, the matrix changes at higher temperatures and evolves from a mixed-matrix (H_2+CO) to a CO matrix. In this way, around 6 K, the CO matrix traps species such as HCO, H_2CO, and few number of H_2 molecules. By annealing the system from 6 to 10 K, species such as $HCO\cdots(H_2)_n$ and $H_2CO\cdots(H_2)_n$ evolve toward isolated monomers, namely, HCO and H_2CO, trapped in a CO matrix. The result is a stepwise decrease in the IR signature of these species. Indeed, the very weak intensity of HCO and H_2CO absorption bands at 10 K means that HCO and H_2CO concentration in the CO matrix become very low, as shown in Figure 5. The shape of the $2\nu_{CO}$ absorption band slightly changes between 6 and 10 K because of H_2 desorption. Nevertheless, its intensity remains relatively constant, CO being the dominant species in this temperature range.

5. Conclusions

The environmental influence on the successive hydrogenation of CO has been studied through the comparison of two types of experiments, hydrogenation of a CO surface and co-injection of (CO + H), monitored at 3 and 10 K. At 10 K, under our experimental conditions, the hydrogenation of a CO surface promotes the formation of stable molecules, such as H_2CO and CH_3OH, whereas the same experiment performed at 3 K yield no product. On the contrary, when H atoms and CO molecules are coinjected, both HCO and H_3CO radicals can be observed at 10 K, in addition to CH_3OH and H_2CO. The codeposition of H + CO performed at 3 K reveals that the HCO radical and H_2CO molecules are the only species to be detected. At this very low temperature, the intensity of H_2CO is lower than that of the HCO radical. Moreover, the co-injection technique highlights the apparition of new species. The formation of these new species and the intermediate species obtained in the reaction of successive hydrogenation of CO seems to depend strongly on both the temperature and the H concentration. The environment in which CO molecules and H atoms get into contact is crucial to the formation of new and/or intermediate species. Quantum calculations and isotopic studies are currently being undertaken to characterize these new species better. Concomitantly, the hydrogenation of CO by co-injection will be subjected to new environmental conditions to better understand the role and evolution of the species involved.

Acknowledgment. This work was supported by CNRS national program PCMI (Physics and Chemistry of the Interstellar Medium) and by the federation SMART (LADIR, LCPMR, LCT). Part of the calculations was performed using HPC resources from GENCI-CINES (grant 2009-085128).

References and Notes

(1) Herbst, E. *J. Phys. Chem. A* **2005**, *109*, 4017.
(2) Teixeira, T. C.; Emerson, J. P.; Palumbo, M. E. *Astron. Astrophys.* **1998**, *330*, 711.
(3) Tielens, A. G. G. M.; Tokunaga, A. T.; Geballe, T. R.; Baas, F. *Astrophys. J.* **1991**, *381*, 181.
(4) Chiar, J. E.; Adamson, A. J.; Kerr, T. H.; Whittet, D. C. B. *Astrophys. J.* **1995**, *455*, 234.
(5) McKellar, A. R. W. *J. Chem. Phys.* **1998**, *108*, 1811.
(6) Noga, J.; Kallay, M.; Valiron, P. *Mol. Phys.* **2006**, *104*, 2337.
(7) Pak, I.; Surin, L. A.; Dumesh, B. S.; Roth, D. A.; Lewen, F.; Winnewisser, G. *Chem. Phys. Lett.* **1999**, *304*, 145.
(8) Jankowski, P.; Szalewicz, K. *J. Chem. Phys.* **2005**, *123*, 104301.
(9) Hidaka, H.; Watanabe, N.; Shiraki, T.; Nagaoka, A.; Kouchi, A. *Astrophys. J.* **2004**, *614*, 1124.
(10) Watanabe, N.; Kouchi, A. *Astrophys. J.* **2002**, *571*, 173–176.
(11) Fuchs, G. W.; Cuppen, H. M.; Ioppolo, S.; Romanzin, C.; Bisschop, S. E.; Andersson, S.; van Dishoeck, E. F.; Linnartz, H. *Astron. Astrophys.* **2009**, *505*, 629.
(12) Stantcheva, T.; Shematovich, V. I.; Herbst, E. *Astron. Astrophys.* **2002**, *391*, 1069.
(13) Hiraoka, K.; Miyagoshi, T.; Takayama, T.; Yamamoto, K.; Kihara, Y. *Astrophys. J.* **1998**, *498*, 710.
(14) Watanabe, N.; Nagaoka, A.; Shiraki, T.; Kouchi, A. *Astrophys. J.* **2004**, *616*, 638.
(15) Zhitnikov, R. A.; Dmitriev, Yu. A. *Astron. Astrophys.* **2002**, *386*, 1129.
(16) Hidaka, H.; Miyauchi, N.; Kouchi, A.; Watanabe, N. *Chem. Phys. Lett.* **2008**, *456*, 36.
(17) Watanabe, N.; Kouchi, A. *Prog. Surf. Sci.* **2008**, *83*, 439.
(18) Hidaka, H.; Kouchi, A.; Watanabe, N. *J. Chem. Phys.* **2007**, *126*, 204707.
(19) Ewing, G. E.; Thompson, W. E.; Pimentel, G. C. *J. Chem. Phys.* **1960**, *32*, 927.
(20) Milligan, D. E.; Jacox, M. E. *J. Chem. Phys.* **1964**, *41*, 3032.
(21) Style, D. W. G.; Ward, J. C. *Trans. Faraday Soc.* **1953**, *49*, 999.
(22) Manceron, L.; Alikhani, M. E.; Tremblay, B. *J. Phys. Chem. A* **2000**, *104*, 3750.
(23) Dunning, T. H. *J. Chem. Phys.* **1989**, *90*, 1007.
(24) Woon, D. E.; Dunning, T. H. *J. Chem. Phys.* **1993**, *98*, 1358.
(25) Wilson, A. K.; Peterson, K. A.; Woon, D. E.; Dunning, T. H. *J. Chem. Phys.* **1999**, *110*, 7667.
(26) Frisch, M. J.; Trucks, G. W.; Schlegel, H. B.; Scuseria, G. E.; Robb, M. A.; Cheeseman, J. R.; Montgomery, J. A., Jr.; Vreven, T.; Kudin, K. N.; Burant, J. C.; Millam, J. M.; Iyengar, S. S.; Tomasi, J.; Barone, V.; Mennucci, B.; Cossi, M.; Scalmani, G.; Rega, N.; Petersson, G. A.; Nakatsuji, H.; Hada, M.; Ehara, M.; Toyota, K.; Fukuda, R.; Hasegawa, J.; Ishida, M.; Nakajima, T.; Honda, Y.; Kitao, O.; Nakai, H.; Klene, M.; Li, X.; Knox, J. E.; Hratchian, H. P.; Cross, J. B.; Bakken, V.; Adamo, C.; Jaramillo, J.; Gomperts, R.; Stratmann, R. E.; Yazyev, O.; Austin, A. J.; Cammi, R.; Pomelli, C.; Ochterski, J. W.; Ayala, P. Y.; Morokuma, K.; Voth, G. A.; Salvador, P.; Dannenberg, J. J.; Zakrzewski, V. G.; Dapprich, S.; Daniels, A. D.; Strain, M. C.; Farkas, O.; Malick, D. K.; Rabuck, A. D.; Raghavachari, K.; Foresman, J. B.; Ortiz, J. V.; Cui, Q.; Baboul, A. G.; Clifford, S.; Cioslowski, J.; Stefanov, B. B.; Liu, G.; Liashenko, A.; Piskorz, P.; Komaromi, I.; Martin, R. L.; Fox, D. J.; Keith, T.; Al-Laham, M. A.; Peng, C. Y.; Nanayakkara, A.; Challacombe, M.; Gill, P. M. W.; Johnson, B.; Chen, W.; Wong, M. W.; Gonzalez, C.; Pople, J. A. *Gaussian 03*, revision C.02; Gaussian, Inc.: Wallingford, CT, 2004.
(27) Shimanouchi, T. *Tables of Molecular Vibrational Frequencies Consolidated*; National Bureau of Standards: Washington, DC, 1972; Vol *5*, pp 1−160.

(28) Schutte, W. A.; Allamandola, L. J.; Sandford, S. A. *Science.* **1993**, *259*, 1143.
(29) Watanabe, N.; Hidaka, H.; Kouchi, A. *AIP Conf. Proc.* **2006**, *855*, 122.
(30) Enhdahl, A.; Nelander, B. *Chem. Phys. Lett.* **1988**, *148*, 264.
(31) Tam, S.; Fajardo, M. E. *Rev. Sci. Instrum.* **1999**, *70*, 1926.
(32) Nelander, B. *J. Chem. Phys.* **1980**, *73*, 1034.
(33) Diem, M.; Lee, E. K. C. *Chem. Phys.* **1979**, *41*, 373.
(34) Hidaka, H.; Kouchi, A.; Watanabe, N. *J. Chem. Phys.* **2007**, *126*, 204707.

JP909600Q